Simulation of Human Diving

by

Wayne L. Wooten and Jessica K. Hodgins

GIT-GVU-94-31
July 1994

Graphics, Visualization & Usability Center

Georgia Institute of Technology
Atlanta GA 30332-0280

Simulation of Human Diving

Wayne L. Wooten and Jessica K. Hodgins
College of Computing
Georgia Institute of Technology
Atlanta, GA 30332-0280
[wlw | jkh]@cc.gatech.edu

Abstract

In this paper we describe a dynamic model and control system for a human platform diver. The dynamic model is a 38 degree-of-freedom rigid body model with dynamic parameters similar to those given in the literature for humans. The control system uses a state machine, algorithms for balance, and proportional-derivative servos to balance the model on a 10 meter platform, to generate the angular velocity for the dive, and to perform the maneuvers required during the dive. The motion of the simulated divers closely resembles video footage of dives performed by human athletes. The control and simulation techniques presented in this paper will be useful for analysis of sports performance and to as a source of realistic motion for synthetic actors.

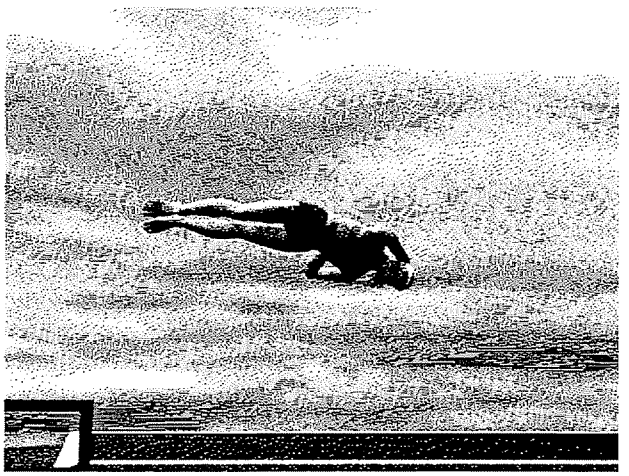

Figure 1: Graphical image of the diver in the flight phase of a backward 1-$\frac{1}{2}$ somersault pike with $\frac{1}{2}$ twist.

Introduction

Capturing the nuances of human motion in animation is a difficult problem with traditional or computer animation techniques. If the motion or appearance of an animated human is unnatural, the audience will find the motion unappealing. Because of the subtleties of human motion and the high standards we apply to the appearance of animated humans, we do not yet have natural and realistic computer animations of many human behaviors.

One potential solution to this problem is simulation and the human motion described in this paper was generated using a rigid body simulation. Dynamic simulation yields motion that is physically correct within the limits of the simulated model because the model takes into account the mass, inertia, and physical laws affecting the motion. Physically correct motion is not necessarily natural-looking motion and dynamic simulation alone will not provide motion for an active system, such as a human, with an internal source of energy. For active systems, control algorithms are used to compute the torques that should be applied at the joints to cause the model to perform the desired task. To produce natural-looking motion, the control algorithms must mimic those used by humans and avoid excessive torques, extraneous motions, and other artifacts that will make the motion appear unnatural.

Dynamic simulations, coupled with control systems, allow an animator to control the action of human models in a high-level and intuitive fashion. With simulation, the motions of individual body parts are computed using the equations of motion and the joint angles do not have to be individually specified. One potential disadvantage of using dynamic simulation is that the animator no longer has explicit control over the absolute location of the joint angles at any given point in time, and therefore is unable to influence the subtleties of the motion directly.

This paper discusses the simulation and control of a human performing several 10 meter platform dives. The dives performed by the animated human are an inward 1-$\frac{1}{2}$ somersault pike, a reverse 3-$\frac{1}{2}$ somersault

tuck, and a backward 1-$\frac{1}{2}$ somersault with $\frac{1}{2}$ twist (figure 1). In this paper, we focus on the generation of a physically realistic, dynamic simulation of a human and on the development of control algorithms for diving. The next section presents related research from areas that provide the foundation for this work. The third section describes the methods used to generate and control the simulation. A discussion of the model and the results we obtained is presented in the last section.

Background

Three areas provide material relevant to the simulation of diving. Results from robotics and control theory have allowed the construction of robots that perform a variety of different tasks and the results provide insight into possible control algorithms for a diving human. The biomechanics literature contains studies of the dynamic properties of the human body as well as analysis of the techniques used for various aerial maneuvers. The computer graphics community has explored many of the problems inherent in modeling and animating humans in a realistic fashion.

Robotics

Research in the area of robotics has focused on the construction and control of mechanical systems. Although a robot with the degrees of freedom of a human body has not yet been built, the methods and techniques used in controlling actual robots in the laboratory are applicable to the simulation of more complex systems. Raibert and his colleagues built a series of running machines that performed a number of dynamic tasks. They developed one, two, and four-legged robots that run, walk, hop, change gaits, and climb stairs (Raibert 1986; Hodgins 1991; Hodgins and Raibert 1991). Of this research, the control algorithms that allowed planar and three-dimensional two-legged robots to perform somersaults are the most relevant to diving. (Hodgins and Raibert 1990; Playter and Raibert 1992). To initiate a somersault, the machine runs forward, thrusts with both legs, and pitches the body forward using the hip actuators. The robot shortens its legs during the somersault to increase angular velocity. The robot lengthens its legs to land, lands on both feet, and continues running. The somersault is similar to a dive in that the creature must apply forces to the ground to generate the needed angular momentum for the ballistic part of the maneuver and the control techniques for the divers build on the control ideas developed for the somersaulting robots.

Murthy and Keerthi (1993) present an optimal control system for a two-dimensional, four degree-of-freedom diver. They formulated a time-optimal control problem using state and control constraints and used a numerical approach to compute the solution. The simulated diver performed both forward and backward somersaults. Solutions required about 10 minutes of computation on an Intel 486-based machine.

Biomechanics

Biomechanics is concerned with the study of human performance as related to the mechanical systems of the body. One area of research is concerned with the techniques and methods used by humans in performing aerial maneuvers. Results from this research provide insight into possible techniques for simulating the human diver. Yeadon and his colleagues analyzed human movement by recording the three-dimensional motion of aerial maneuvers with high-speed film cameras and digitizing the resulting footage (Yeadon 1990; Yeadon, Athia, and Hales 1990). Yeadon also developed a dynamic model of the human body and a simulation system for aerial maneuvers. Yeadon's system used inverse dynamics without a control system, in contrast to our diving simulation which uses forward dynamics with a control system. The data from film capture for three test subjects compared favorably with Yeadon's simulation.

For many years, researchers have debated how cats land on their feet and how humans perform certain free-fall aerial maneuvers. Frohlich presents an excellent discussion of the techniques used by humans for aerial maneuvers (Frohlich 1979). He describes the physical characteristics of divers and dives and uses this as a basis for describing different techniques for initiating somersaults and twists. Through simulation and informal human experiments, he demonstrated how humans can perform somersaults and twists using torque generated by pushing on a platform and also showed how they can perform similar maneuvers with no angular momentum from the platform.

Computer Animation

Animation of human motion has long been a major focus of research in the graphics community. Girard (1987) developed models of articulated figure motion using a hybrid kinematic/dynamic approach. The overall position and trajectory of the body was modeled dynamically, but the position of each limb was controlled kinematically. Wilhelms (1987) also developed dynamic simulations of articulated human fig-

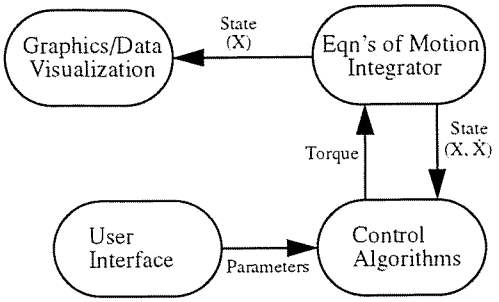

Figure 2: A diagram of the animation system used for the dynamic simulation of human models. The user controls the animation by providing parameters for the control system, such as the amount of twist during lift-off. The control system uses this information to compute a torque for the integrator. The equations of motion are used to compute the acceleration for a given torque and state of the system. The integrator computes the velocity and position at the next time step by integrating the acceleration. The system state is then used to draw the graphical image and provide feedback for the control system.

ures, using user-specified torques at each joint to provide control.

The Jack system developed by Badler and his colleagues incorporates kinematic and dynamic models of humans based on data collected by NASA (Badler et al 1993). The system allows the body to be positioned interactively and has several built-in behaviors including balance, reaching, grasping, and a walking behavior that uses a simplified dynamic model. In addition, they developed a model of human motion based on the strength profiles for a range of motion corresponding to each joint (Lee et al 1991). Jack has been used extensively for ergonomic analysis and human factors engineering.

Magnenat-Thalmann, Thalmann, and colleagues explored methods for simulating and rendering realistic representations of human figures. They focused on facial animation, animation of clothing and hair, and skin deformation (Magnenat-Thalmann 1989; Carignan et al 1992; Magnenat-Thalmann and Thalmann 1990; Gourret, Magnenat-Thalmann, and Thalmann 1989).

Simulation of Human Diving

The system used to create the animations of a diving human consists of the equations of motion for a rigid body model of a human, control algorithms for diving, a graphical display for viewing the motion, and a user interface for changing the parameters of the simulation (figure 2). The user directs the simulation by specifying desired characteristics for the dive. For example, the animator might specify when and how tightly the diver should bend at the waist. At each simulation time step, the control system computes torques for each joint based on the state of the system and the requirements of the task. The equations of motion of the system are integrated forward in time, and the resulting motion is displayed using a graphical model and recorded for later use. The details of the human model and control system are described below.

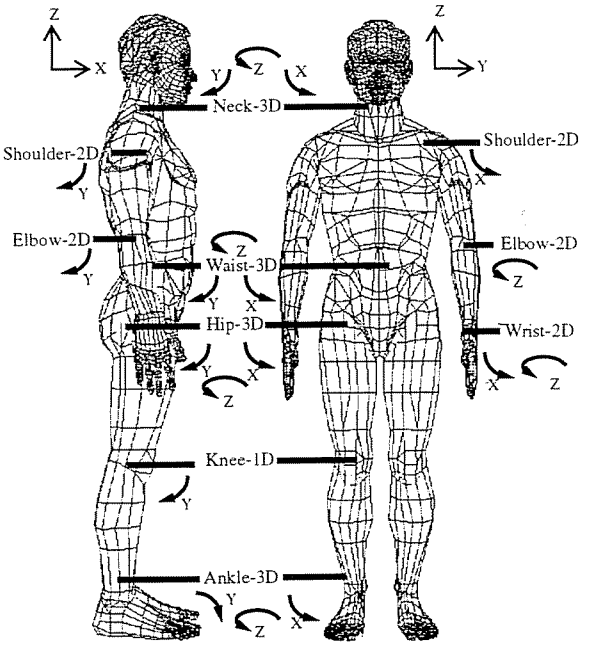

Figure 3: The controlled degrees of freedom of the human model. There are fourteen joints and the diagrams shows the number of degrees of freedom at each joint. The direction of the arrows indicate the positive direction of rotation for each degree of freedom. The polygonal model was obtained from Viewpoint Datalabs.

Model

The human is approximated by a rigid-body model consisting of 15 segments connected by rotary joints. Some joints, like the knee, are modeled as a single axis pin joint, others are modeled by two and three axis gimbal joints. The volume, mass, center of mass, and moments of inertia are calculated from a polygonal representation of the human body (figure 3). The algorithm used to calculate the properties of the polygonal model integrates technique over the set of tetrahedra formed by the triangular faces of the model and the origin. (Lien and Kajiya 1984). Density data obtained from anatomical literature was used in calcu-

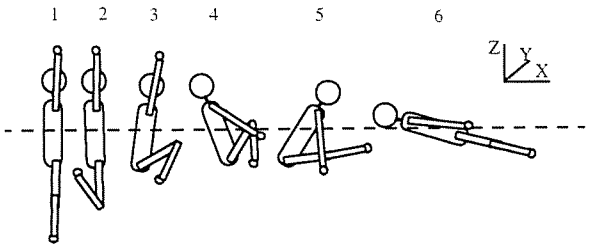

Figure 4: A back-flip can be performed by a human with no angular velocity by moving the limbs of the body in the order shown in this diagram.

Link	Density (g/cm^3)	Mass (kg)	Moment of Inertia (x, y, z kgm^2)		
Head	1.1708	5.89	0.030	0.033	0.023
Torso	1.0088	29.27	0.73	0.63	0.32
Pelvis	1.0297	16.61	0.23	0.18	0.16
Upper Leg	1.0401	8.35	0.15	0.16	0.025
Lower Leg	1.0789	4.16	0.055	0.056	0.007
Foot	1.0664	1.34	0.0018	0.0075	0.0070
Upper Arm	1.0676	2.79	0.025	0.025	0.0050
Lower Arm	1.1015	1.21	0 .0050	0.0054	0.0012
Hand	1.0696	0.551	0.0016	0.0020	0.0005

Table 1: Parameters of the rigid body model of a human. The moment of inertia is computed about the center of mass of each link. The densities are given in Dempster and Gaughran (1965).

Link	COM to Proximal (x, y, z m)			COM to Distal (x, y, z m)		
Torso to neck				.012	0	.32
Torso to waist				.012	0	-.22
Torso to shoulder				-.048	±.164	.12
Head	-.009	0	-.064			
Pelvis	.023	0	.103	.005	±.098	-.11
Upper Leg	.024	±.006	.120	-.052	±.019	-.21
Lower Leg	.005	±.019	.165	-.002	±.009	-.25
Foot	-.046	±.009	.048			
Upper Arm	-.0002	±.056	.120	-.005	±.036	-.17
Lower Arm	-.025	±.007	.090	.012	±.014	-.11
Hand	-.026	0	.085			

Table 2: The distance from the center of mass of each link to the distal and proximal joints in x, y, and z. The positive distance along the Y-axis refers to a location on the left side of the body, while a negative distance refers to the right side.

lating the dynamic properties of the body segments (Dempster and Gaughran 1965). The densities can be found in table 1, and we assume that the density of each body part is uniform. The mass of the dynamic model, computed using the polygonal model, is similar to measurements from cadavers (Dempster and Gaughran 1965). We also tested the dynamic accuracy of the model by making it perform a back-flip maneuver without the presence of angular momentum (Frohlich 1979). The back-flip caused our model to rotate 70° while Frohlich's model performed an 82° back-flip (figure 4).

The graphical image used to monitor the behavior of the model is shown in figure 1, the parameters of the model are given in table 1, and the degrees of freedom of the joints are shown in figure 3. The equations of motion were generated using a commercially available package, that generates subroutines for the equations of motion using a variant of Kane's method and a symbolic simplification phase (Rosenthal and Sherman 1986).

The dynamic interaction of the diver's feet with the platform is modeled using three-dimensional constraints. Each dive involves either two or four points of contact for each foot, depending on whether the ball of the foot or both the ball and the heel are on the platform. The acceleration of the contact point of the foot with respect to the platform is the constraint error. The forces computed with the constraint matrix are applied to the foot at the point of contact. The penetration of the foot into the platform and the velocity of the foot relative to the platform are used to stabilize the constraint equations using Baumgarte stabilization (Baumgarte 1972). To allow the feet to leave the platform, the force is applied to the foot only when the foot has penetrated the platform a specified amount and the velocity of the foot is in the same direction as that of gravity. Friction is infinite in this simulation, so the diver cannot slip on the platform.

In addition to using constraints for contact with the platform, constraints are also used by the somersaulting diver to achieve a tight tuck. For the somersaulting dive, the diver pulls his legs to his chest with his hands. A distance constraint is used to constrain the diver's hands to his knees. Much like the platform constraint, the relative acceleration of the hands and knees are used to compute the force that should be applied to each body. The force applied to the hands is equal and opposite to that applied to the knees.

Control of Diving

To perform a platform dive, a human must take different control actions during the different phases of the dive. For example, during somersaulting dives divers first bend their knees and push from the platform with their feet. Once a diver is in the air he or she will pike or tuck at the waist to perform the somersault. Finally before entering the water divers will straighten, placing their arms over their head. We reproduce this behavior in simulation by using a state machine to select the type of control needed for each phase of the

State	Inward 1-$\frac{1}{2}$ somersault	Reverse 3-$\frac{1}{2}$ somersault	Backward 1-$\frac{1}{2}$ twist
Compression	Prepare for jump: Bend at Knees +Y Bend at Hips -Y	Prepare for jump: Bend at Knees +Y Bend at Hips -Y Swing Arms behind Back	Prepare for jump: Bend at Knees +Y Bend at Hips -Y Swing Arms behind Back
Decompression	Jump from platform: Bend at Waist -Y Straighten Hips Straighten Knees Swing Arms down Extend Ankles and push off platform	Jump from platform: Bend at Waist +Y Straighten Hips Straighten Knees slightly Swing Arms over Head Extend Ankles and push off platform	Jump from platform: Bend at Waist +Y Twist at Waist +Z Straighten Hips Straighten Knees Swing Arms forward Extend Ankles and push off platform
Flight1	Perform pike: Bend at Hips -Y	Perform tuck: Bend at Hips -Y Bend at Waist -Y Bend at Knees +Y Bring Arms down to Knees	Perform twist: Untwist at Waist -Z Twist at Waist +X Bring Left Arm over Head Bring Right Arm across Chest
Flight2		Perform tight tuck: Constrain Hands to Knees	Perform pike: Bring both Arms to Sides Untwist at Waist -X Bend at Waist -Y Bend at Hips -Y
Entry	Prepare to enter water: Straighten Hips Swing Arms over Head	Prepare to enter water: Straighten Hips Straighten Knees Straighten Waist Swing Arms over Head	Prepare to enter water: Straighten Hips Straighten Waist Swing Arms over Head

Table 3: The state machine determines which control laws should be in effect to perform the specified task at each phase of the dive. The axis of rotation of a joint correlates to figure 3. Figure 5 shows an image sequence for each dive in this table.

dive. The main phases of the dive are *Compression*, *Decompression*, *Flight1*, *Flight2*, and *Entry*. While the basic phases are common to all dives, different dives will require different control actions at each phase. For example, during the *Flight1* phase, a twisting diver will activate control actions to twist at the waist, but a somersaulting diver will bend at the waist instead. The transitions are based upon a global clock that is initiated at the start of the dive.

The control laws for the three dives are presented in table 3. In the *Compression* phase the simulated diver bends his knees, hips, and ankles in preparation for the dive. In the *Decompression* phase, the diver straightens his hips and knees, while pushing off the platform with his ankles. During *Decompression* the arms swing to generate the appropriate angular velocity for a twisting or somersaulting dive. In *Flight1* and *Flight2* the diver performs the desired maneuver. The *Entry* phase occurs when the diver straightens, puts his arms over his head, and enters the water.

During the dive, multiple levels of control are active. For example, during lift-off three levels of control are active. The highest level of control is the state machine that detects the time-based transition from *Compression* to *Decompression*. The middle level of control maintains balance by setting the desired position of the ankle proportional to the position of the knee:

$$ankley_{\mathrm{d}} = ankley_{\mathrm{nom}} + 0.2kneey_{\mathrm{d}}$$

where $ankley_{\mathrm{d}}$ is the desired angle about the Y-axis for the ankle, $ankley_{\mathrm{nom}}$ is the nominal position of the ankle, and $kneey_{\mathrm{d}}$ is the desired angle about the Y-axis for the knee. The lowest level of control positions each joint at its desired position using a proportional-derivative servo:

$$\tau = k_p(\phi_d - \phi) + k_v\dot{\phi}$$

where τ is the torque computed for the joint, ϕ is the joint location, ϕ_d is the desired joint location, and $\dot{\phi}$ is the joint rotation rate. The gains of the proportional-derivative servo, k_p and k_v, were chosen empirically (table 4). The desired values are smoothed by using trajectories to go from the current desired value to the newly computed desired value. Eliminating large step changes in the desired values reduces the jerk seen in the simulated motion.

We simulated three different dives using this control framework. The inward 1-$\frac{1}{2}$ somersault pike is the least difficult dive to perform, because the somersault does not require a large angular velocity and the diver has a large window of time to prepare for entry into the

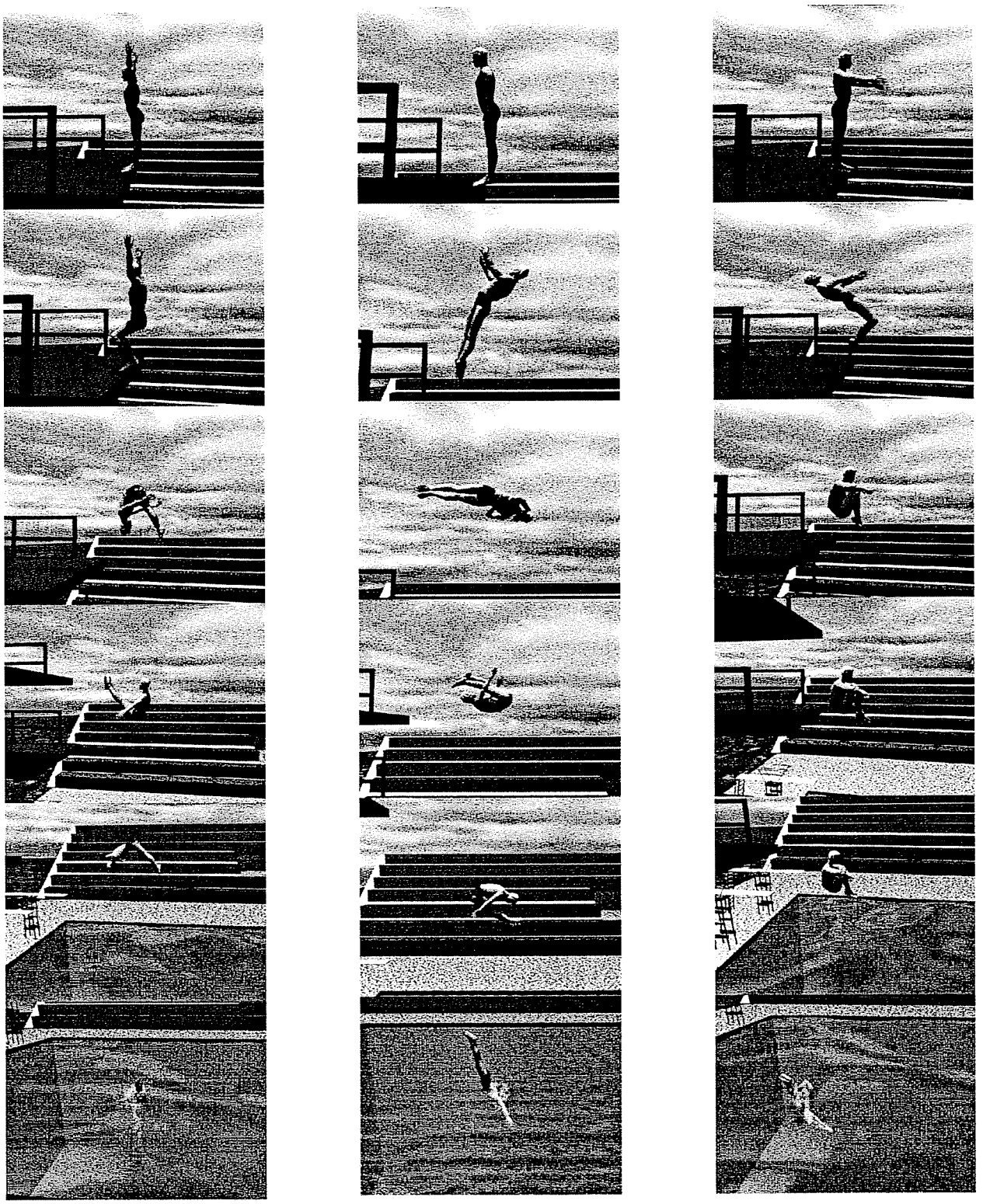

Figure 5: A sequence of images from the three simulated dives. The inward 1-$\frac{1}{2}$ somersault pike is on the left, the backward 1-$\frac{1}{2}$ somersault pike with $\frac{1}{2}$ twist is in the center, and the reverse 3-$\frac{1}{2}$ somersault tuck is on the right. Each image in each sequence is separated by 0.5 seconds in time. In the reverse 3-$\frac{1}{2}$ somersault tuck the diver is at the beginning of each somersault in frames 3, 4, and 5.

Joint	Proportional x,y,z Gain			Derivative x,y,z Gain		
$Neck^{PST}$	30	30	30	3	3	3
$Waist^{PST}$	450	450	450	30	50	30
$Waist^{S}$ (flight)	450	600	450	30	50	30
$Waist^{S}$ (entry)	450	450	450	30	50	30
$Waist^{T}$ (flight)	450	600	1000	30	50	100
Hip^{PST}	100	200	40	10	20	4
Hip^{S} (flight)	100	200	70	10	20	7
Hip^{S} (entry)	100	100	70	10	20	7
Hip^{T} (flight)	200	100	200	20	20	20
$Knee^{PST}$		400			20	
$Knee^{PS}$ (decomp)		900			20	
$Knee^{T}$ (decomp)		600			20	
$Ankle^{PST}$	200	200	20	3	7	1
$Shoulder^{PST}$	60	60		7	7	
$Shoulder^{S}$ (flight)	80	100		8	8	
$Elbow^{PST}$		40	20		4	1
$Wrist^{PST}$	10		1	1		0.1

Table 4: Gains used for the proportional-derivative servos on each joint. For some joints, the gains depend on the type of dive and state of the system. The superscript P denotes a 1-$\frac{1}{2}$ somersault pike, S denotes a 3-$\frac{1}{2}$ somersault tuck, and T denotes a 1-$\frac{1}{2}$ somersault with $\frac{1}{2}$ twist. The gains for the waist and hip increase to allow the diver to perform the specified maneuver. Also note the shoulder increases gain for the somersault, so they can pull the knees to the chest in the flight phase.

water. Graphs of the angular velocity for this dive are shown in figure 6. The graph shows that the angular velocity for the inward 1-$\frac{1}{2}$ somersault pike rises slowly, remains nearly constant for the duration of flight and then drops upon entry into the water. An image sequence of this dive is shown in figure 5.

The second dive is a reverse 3-$\frac{1}{2}$ somersault tuck. This dive is more difficult than the 1-$\frac{1}{2}$ somersault because the required angular velocity is much larger and a very tight tuck is required during the flight phase to achieve such a high angular velocity. Human divers use their hands to pull their knees close to their chest and we used the constraints mentioned earlier to attach the hands of the simulated diver to his knees. The constraints allowed the simulation to achieve the inertial configuration needed to generate the high angular velocity for this dive. A graph of the angular velocity about the somersaulting axis for this dive is shown in figure 6. The graph shows that the rotation for this dive is in the opposite direction from that needed in the inward and backward dive. The data also shows that the 3-$\frac{1}{2}$ somersault requires much more angular velocity than the other two dives. An image sequence of this dive is shown in figure 5.

The backward 1-$\frac{1}{2}$ somersault with $\frac{1}{2}$ twist was the most difficult dive to control because it involved rotations about multiple axes. However, this dive is rated as an easier dive for humans than the 3-$\frac{1}{2}$ somersault

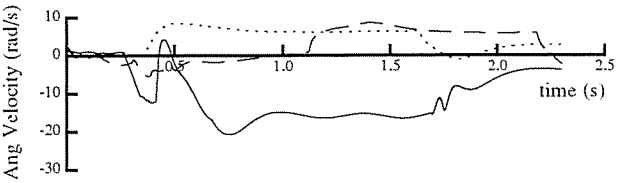

Figure 6: Graphs of the angular velocity about the somersaulting axis for all three dives. The 3-$\frac{1}{2}$ somersault is represented by a solid line, the 1-$\frac{1}{2}$ somersault by a dotted line, and the $\frac{1}{2}$ twist by a dashed line.

because the rotation rate is lower. This dive requires the generation of twisting torque at lift-off, and the transferal of angular velocity about the twist axis to angular velocity about the somersaulting axis. The technique used to transition from a twist to a somersault is presented in Frohlich (1979). Divers having non-zero angular momentum and performing a somersault about the X-axis can initiate a twist by throwing their left arm down and their right arm up. This motion results in a counterclockwise rotation of the diver about the Y-axis. This rotation causes a twisting motion about the Z-axis because the diver's principal axes of rotation are no longer aligned with their angular momentum axis, so the angular velocity vector now has components along both the X and Z-axis. Figure 7 shows a diagram of this technique, and figure 8 shows the rates of rotation about all three axes and the location of the diver over time for the twisting dive. The location of the center of mass follows a parabola because the diver is falling under the influence of gravity. The graphs of the location of the center of mass for the other two dives look very similar, except the diver skews in the Y direction more during a twisting dive. The graph of the angular velocity shows that the angular velocity is highest about the twisting axis during the first half of the dive, but decreases as the angular velocity about the somersaulting axis increases. Figure 8 also shows the movement of the hip and waist. The dashed line indicates the desired value for the joint computed by the control system and the solid line indicates the actual motion of the joint.

Discussion

Images of the backward 1-$\frac{1}{2}$ somersault with $\frac{1}{2}$ twist, performed by a simulated diver and a human diver, are shown in the image sequence in figure 9. Each simulated dive was compared to video footage of Olympic athletes performing the same dive by compositing the simulated dive and the actual dive side by side on video and synchronizing the dives at the point in time when

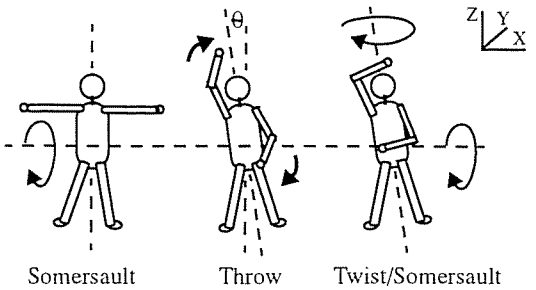

Figure 7: As a somersaulting diver brings one arm over their head and one arm to their side they induce a rotation about the Y-axis. If the diver had non-zero angular momentum, a twist would be induced about the Z-axis in order to conserve angular momentum. Because the rotation of θ, their body-local X-axis is no longer aligned with the angular momentum axis and their body begins to twist.

both divers entered the water. The simulated diver does not perform the dive in exactly the same manner as the real athlete because he leaves the platform more quickly, but takes more time to transition from twist to somersault. The simulated diver and human diver perform the pike and entry phases in a similar fashion.

Despite the natural-looking motion achieved with the model of the diver, many simplifying assumptions were made in the model. We assumed that air resistance was negligible and did not apply drag to the body as it fell through the air. While not correct, this assumption does not affect the motion of the diver substantially because they fall at a maximum velocity of 15 m/s and at that velocity air resistance does not slow the diver significantly (Van Gheluwe 1981). We also assumed that the density of each body part of the human model was uniform and that the joints were simple revolute joints. Despite the assumption of uniform density the moments of inertia are similar to human data from Dempster and Gaughran (1965). The assumption of simple revolute joints does influence the motion however, and a more accurate model of the shoulder and spinal column, such as those used in the Jack system (Badler 1993), would make the motion look more natural.

Joint range limitations and strength considerations were not taken into account in our model. The force at each joint comes from a torque source placed at that joint and this simplification could result in a simulated human that is stronger or faster than a real human. If the gains on the control system are too high, the resulting motion will be unnatural. For example, a dive might be performed that met the specifications, in that the diver tucked, opened, and entered the water vertically, but the performance might lack the grace and style of a human one. Although the accuracy of

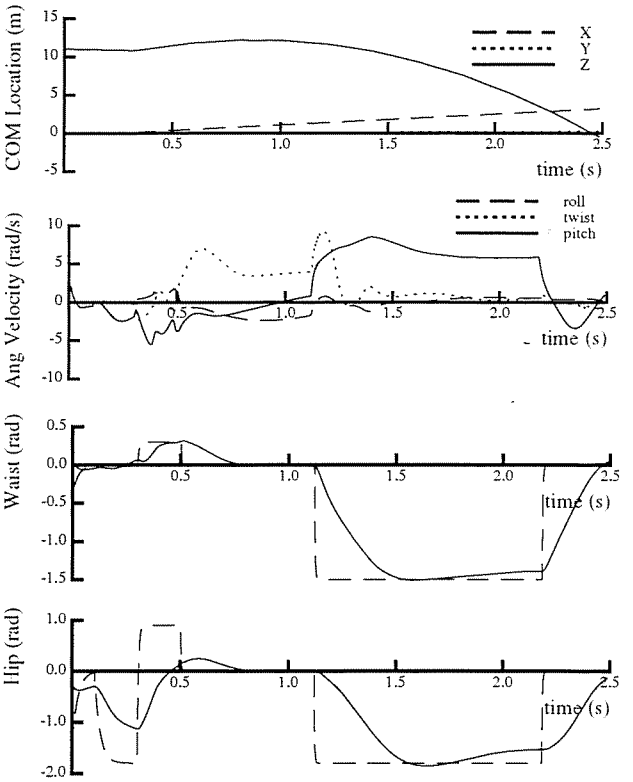

Figure 8: Graphs of the location of center of mass, angular velocity, and selected joint motion for the $\frac{1}{2}$ twist dive. The dashed lines in the last two graphs represent the desired location of a joint, and the solid lines represent the actual location.

this simulation is sufficient for computer animation, other applications such as sports performance analysis may require additional accuracy.

The graphical representation of a human influences the observer's perception of the motion. For example, when motion capture data of walking is played back as a series of light sources at each joint, the resulting animation gives observers the impression of a human walking (Johansson 1973). However mapping the same data to a polygonal approximation of a human body raises the audience's expectations and allows them to see more of the motion. Now the audience has a better understanding of motion of the model, and if the motion capture data is inaccurate, then the motion will look less realistic.

A similar effect occurs when we increase the realism of the polygonal representation of the simulated diver. Although the rigid body motion is similar to that of a human diver, our simulation is missing the subtle secondary motion of subsystems of the human body, such as clothing and hair moving in response to the motion of the human body and skin moving in response to muscle contraction. The physical appearance of our

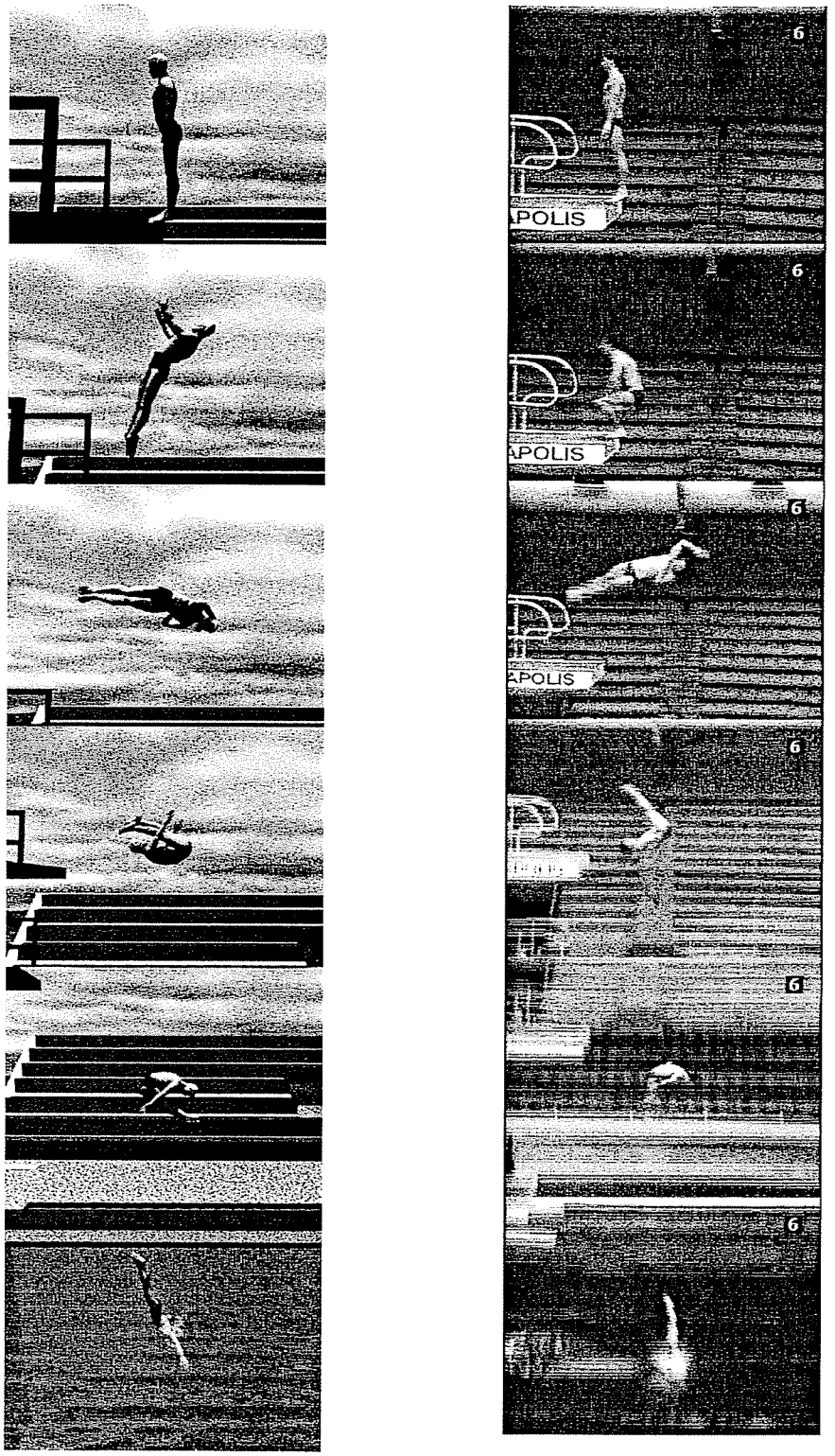

Figure 9: A sequence of images of a simulated diver and a human diver performing a backward 1-$\frac{1}{2}$ somersault pike with $\frac{1}{2}$ twist. Each image is separated by 0.5 seconds in time. The size of the splash is a major consideration in the performance of the dive. This simulation integrates the motion of the diver and a simulation of splashing fluid (O'Brien and Hodgins 1994).

model could be improved with the introduction of a flexible torso, muscle, skin, hair, and clothing, all of which will require additional physical models.

The control system described in this paper works well for the three 10 meter dives. Development of additional dives would require the specification of control actions for the new dives. For example, a 10 meter inward 2-$\frac{1}{2}$ somersault pike would require generation of more angular velocity than the 1-$\frac{1}{2}$ somersault and the actions for each phase would have to be revised.

The control system would have to be tuned for a model of a human with different dynamic parameters. A control system that took action to adjust the amount of rotation during flight would make the diving control system more robust to changes in the dynamic model. A control system that alters rotation during flight in somersaulting robots was developed by Playter and Raibert (1992) and could be adapted to diving. However, the sensor requirements for such a control system might exceed the perceptual information available to a human performing diving maneuvers.

Development of a diver that makes a running approach would require significant work because a separate control system for running would have to be integrated into the diving simulation. Diving from a springboard would require the simulation and integration of a flexible beam into the simulation. Both additions would also require the development of control algorithms for running, walking, and balancing on flexible surfaces.

Diving is a dynamic, acyclic behavior with distinct phases and the control system we designed reflects these properties. Cyclic behaviors like running may require more sophisticated control algorithms because of the need to repeat the pattern with little variation on each cycle (Hodgins 1994). Other human behaviors such as grasping an object or reclining in a chair are acyclic and do not rely as heavily on the dynamics of the system. The state machines described in this paper are less likely to be useful for tasks of this nature.

If dynamic simulation of human motion is to be useful in virtual environments and sports training, the simulations must run in real time. Current workstation graphics hardware can render complex models at the interactive rates needed for virtual environments, but workstation class machines cannot calculate the dynamics of a high degree-of-freedom human model in real time. Our simulation of the human diver with 38 degrees-of-freedom and 24 constraints runs 40 times slower than real time, without graphics, on a Silicon Graphics Onyx with a 150 MHz R4400 processor. We define real time to mean that simulation time equals the time elapsed on a wall clock. With the current rate of increase in speed of workstation hardware and research into faster or parallel dynamics algorithms, the simulation of a realistic rigid body model of a human should run in real time within a few years.

Realistic simulation of human motion will be useful in entertainment, virtual environments, and also has the potential to be useful in athletic performance and human motion studies. Currently, virtual actors are used mainly in entertainment and many examples of their use can be seen in the film, video game, and amusement park industries. Another promising application of techniques for generating realistic human motion is in the area of athletic performance. When analyzing a particular motion, athletes and coaches would be able to change parameters in a physical simulation of a human performing their sport. This ability would allow athletes, who might not understand how the motion of a particular body part will affect their performance, to experiment and ask questions such as, "What if I tucked tighter in this dive?" Interactive simulations could give both coaches and athletes better intuition about the physics involved in their sport and could lead to improved human performance.

Acknowledgments

We would like to thank the US Diving for allowing us to use footage of Olympic athletes, and James O'Brien for integrating his splashing fluid simulation with the diving simulation. This project was supported in part by NSF Grant No. IRI-9309189 and funding from the Advanced Research Projects Agency.

References

Badler, N. I., Phillips, C. B., Webber, B. L. 1993. *Simulating Humans* Oxford: Oxford University Press.

Baumgarte, J., 1972. Stabilization of Constraints and Integrals of Motion in Dynamical Systems. *Computer Methods in Applied Mechanics and Engineering* 1:1–16.

Carignan, M., Yang, Y., Magnenat-Thalmann, N., Thalmann, D., 1992. Dressing Animated Synthetic Actors with Complex Deformable Clothes. *Computer Graphics* 26(2):99–104.

Dempster, W. T., Gaughran, G. R. L. 1965. Properties of Body Segments based on Size and Weight. *American Journal of Anatomy* 120: 33–54.

Frohlich, C. 1979. Do springboard divers violate angular momentum conservation? *American Journal of Physics* 47:583–592.

Girard, M., 1987. Interactive Design of 3D Computer-Animated Legged Animal Motion. *IEEE Computer Graphics and Applications* 7(6):39–51.

Gourett, J., Magnenat-Thalmann, N., Thalmann, D., 1989. Simulation of Object and Human Skin Deformations in a Grasping Task. *Computer Graphics* 23(3):21–30.

Hodgins, J. K. 1991. Biped Gait Transitions. In *Proceedings of the IEEE International Conference on Robotics and Automation*, Sacramento, CA, pp2092–2097.

Hodgins, J., Raibert, M. H. 1990. Biped Gymnastics. *International Journal of Robotics Research*, 9(2):115–132.

Hodgins, J. K., Raibert, M. H. 1991. Adjusting Step Length for Rough Terrain Locomotion. *IEEE Transactions on Robotics and Automation* 7(3):289–298.

Hodgins, J. K., 1994. Simulation of Human Running. *IEEE Conference on Robotics and Automation.* San Diego, CA, pp1320–1325.

Johansson, G., 1973. Visual perception of biological motion and a model for its analysis. *Perception and Psychophysics.* 14(2):201–211.

Lee, P., Wei, S., Zhao, J., Badler, N.I. 1990. Strength Guided Motion. *Computer Graphics* 24(4):253–262.

Lien, S., Kajiya, J. T. 1984. A Symbolic Method for Calculating the Integral Properties of Arbitrary Nonconvex Polyhedra. *IEEE Computer Graphics and Applications* 4(5):35–41.

Magnenat-Thalmann, N. 1989. The Problematics of Facial Animation. *State-of-the-art in Computer Animation* New York: Springer-Verlag, pp.47–58.

Magnenat-Thalmann, N., Thalmann, D. 1990. *Computer Animation: Theory and Practice* New York: Springer-Verlag.

Murthy, N., Keerthi, S. 1993. Optimal Control of a Somersaulting Platform Diver. *IEEE Conference on Robotics and Automation*, Atlanta, GA, pp1013–1018.

O'Brien, J., Hodgins, J. K., 1994. Dynamic Simulation of Splashing Fluids. Georgia Institute of Technology Graphics, Visualization, and Usability Center Technical Report GIT-GVU-94-32.

Playter, R. R., Raibert, M. H. 1992. Control of a Biped Somersault in 3D. In *Proceedings of the IEEE International Conference on Robotics and Automation*, Raleigh, NC, pp582–589.

Raibert, M. H. 1986. *Legged Robots That Balance.* Cambridge: MIT Press.

Rosenthal, D. E., Sherman, M. A., 1986. High Performance Multibody Simulations Via Symbolic Equation Manipulation and Kane's Method. *Journal of Astronautical Sciences* 34(3):223–239.

Van Gheluwe, B., 1981. A biomechanical simulation model for airborne twist in backward somersaults. *Journal of Human Movement Studies* 7:1–22.

Wilhelms, J., 1987. Toward Automatic Motion Control. *IEEE Computer Graphics and Applications* 7(4):11–22.

Yeadon, M. R., 1990. The Simulation of Aerial Movement-I,II,III. *Journal of Biomechanics* 23(1):59–83.

Yeadon, M. R., Atha, J., Hales, F. D., 1990. The Simulation of Aerial Movement-IV. *Journal of Biomechanics* 23(1):85–89.